Poloidal $E \times B$ Drift Used as an Effective Rotational Transform to Achieve Long Confinement Times in a Toroidal Electron Plasma

M. R. Stoneking, M. A. Growdon, M. L. Milne, and R. T. Peterson

Department of Physics, Lawrence University, Appleton, Wisconsin 54911, USA

(Received 10 September 2003; published 4 March 2004)

Electron plasmas with mean densities of 5.0×10^6 cm^{-3} have been confined for as long as 18 ms in a partially toroidal trap with a purely toroidal magnetic field ($B_0 = 196$ G, $R_o = 43$ cm, $a = 5$ cm). Confinement is limited to 2.0 ms unless feedback is employed to suppress the growth of a toroidal version of the $m = 1$ diocotron mode. The confinement time is much longer than all characteristic single-particle drift time scales and therefore confirms the existence of an equilibrium in which the space-charge-generated $\mathbf{E} \times \mathbf{B}$ drift acts as an effective rotational transform.

DOI: 10.1103/PhysRevLett.92.095003 PACS numbers: 52.27.Jt, 52.55.Hc, 52.55.Dy

Quasineutral plasmas cannot be confined in a purely toroidal magnetic field: curvature and ∇B drifts quickly carry particles out of the trap vertically. Vertical drifts are managed and confinement achieved in toroidal plasmas (e.g., in tokamaks) by employing a rotational transform or poloidal component of the magnetic field. Non-neutral plasmas (i.e., plasmas with a single sign of charge [1]), on the other hand, are predicted to exhibit stable equilibria in a purely toroidal magnetic field [2–7]. A handful of electron plasma experiments over more than three decades generally support these predictions, but they fail to confine plasmas for more than about 100 μs [8–14]. The hope of establishing toroidal equilibrium for non-neutral plasmas rests on the poloidal $\mathbf{E} \times \mathbf{B}$ rotation (arising from the space-charge electric field) acting as an effective rotational transform. The experiments described in this Letter successfully exploit a novel partially toroidal trapping strategy to achieve confinement times as long as 18 ms and show, for the first time, unambiguous evidence for the existence of a toroidal equilibrium state for electron plasmas. Other electron plasma experiments presently operating [15,16] or under construction [17] are toroidal in geometry, but the experiment described here is the only contemporary device having a purely toroidal magnetic field ($B = 196$ G at $R_0 = 43$ cm), and thus is the only one suited to testing the effectiveness of poloidal rotation in establishing equilibrium.

By restricting the confinement region to a 300° toroidal arc, controlled and rapid charge injection along field lines is achieved (Fig. 1). The experiment is operated in the same manner as cylindrical Penning-Malmberg experiments [18]. Appropriately timed gate potentials are applied to the trapping grids to execute a load, trap, dump sequence. Electrons emitted from a spiral tungsten filament ($a \approx 5$ cm) stream along the magnetic field into the confinement region during the load phase of the cycle. During the trapping phase, electrons do not circulate toroidally, but execute bounce motion between the toroidally separated (and negatively biased) trapping grids, in addition to undergoing cyclotron motion and $\mathbf{E} \times \mathbf{B}$ drift rotation in the poloidal plane. The plasma is then dumped onto a positively biased phosphor screen and a charge-coupled device (CCD) camera captures the image. Charge collected by the phosphor screen is measured with a capacitively coupled circuit and the grid transparency for electrons is taken to be the same as the optical transparency (52%). By varying the duration of the trapping phase and observing the changes in the total charge collected during the dump, the confinement time is determined.

Nondestructive measurement of trapped plasma dynamics is accomplished by monitoring the flow of image charge to and from a set of four wall patch probes in response to motion of the charged plasma. The probes are connected to the grounded vacuum chamber through a 12 kΩ current-sampling resistor and have a bandwidth

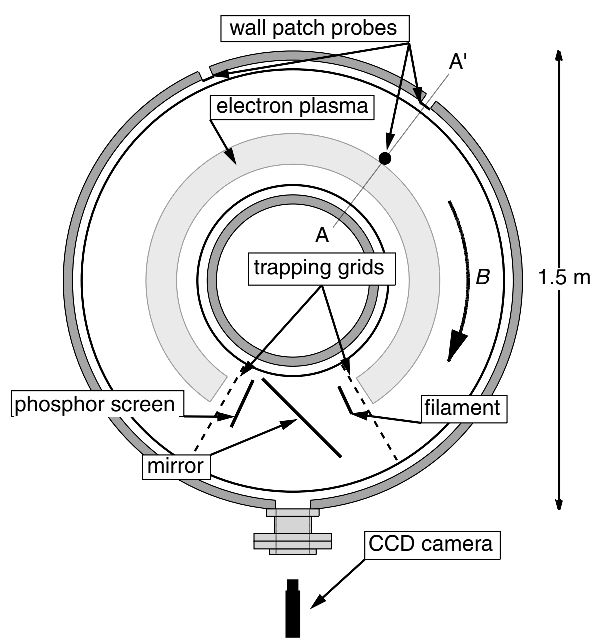

FIG. 1. A top view schematic diagram of the partially toroidal trap.

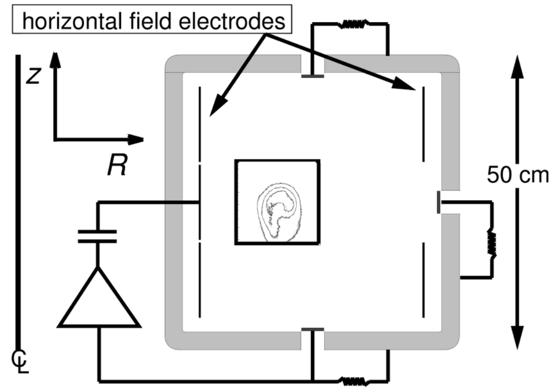

FIG. 2. A schematic diagram of the poloidal cross section A-A′ from Fig. 1 with the projected location of the phosphor screen.

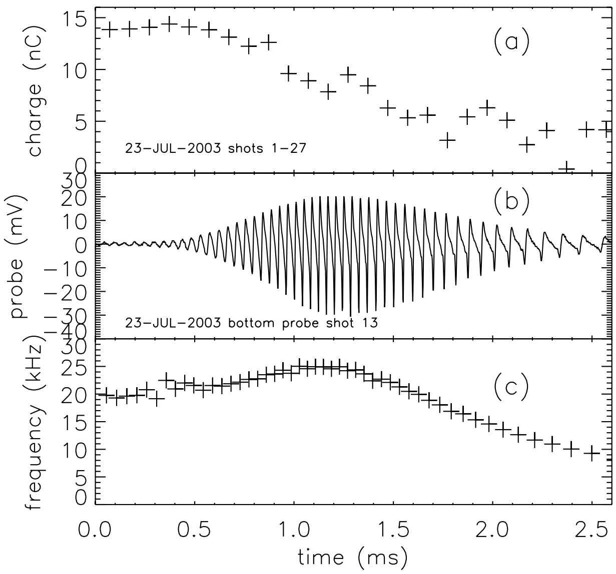

FIG. 3. (a) The trapped charge determined from the charge collected by the phosphor screen during dump. (b) The raw signal on the bottom wall patch probe for a typical shot when the plasma is dumped later than 2.5 ms. (c) The frequency of the wall probe signal versus time for the same shot shown in panel (b).

greater than 1 MHz. Figure 2 shows the relative locations of three probes in the poloidal plane (section A-A′ in Fig. 1) as well as the projected location of the phosphor screen with a representative intensity contour plot derived from the image of a dumped plasma. Also shown in Fig. 2 are five toroidally continuous *horizontal field* electrodes, three hugging the inner wall and two located near the outer wall. By appropriate biasing of the electrodes, an electric field can be applied to the plasma as theory predicts is necessary to achieve a stable equilibrium [6]. In the experiments reported here the vacuum electric field in the vicinity of the plasma is 60 V/m, directed away from the major axis and decreases in magnitude with increasing R.

Typical confinement results are displayed in Fig. 3(a). An initial trapped charge of 14 nC decays by a factor of 2 in 1.4 ms. Confinement in excess of 1 ms represents a record for electron plasmas in devices with a purely toroidal magnetic field, and by itself, would signal successful application of poloidal rotation as a means of establishing toroidal equilibrium. However, we are able to enhance the confinement by another order of magnitude as described below. The mean electron density and maximum space-charge potential implied by the 14 nC initial charge are $5.0 \times 10^6\ \mathrm{cm}^{-3}$ and approximately -56 V, respectively. The space-charge potential is about half the radial potential drop across the spiral filament.

Diocotron oscillations with poloidal mode number $m = 1$ are unambiguously observed in the experiments described here. Figure 3(b) shows the raw signal from one of the wall patch probes during a single shot in which the trapping time exceeded 2.5 ms. The oscillation grows in amplitude, saturates at about 1.3 ms, and then decays both in amplitude and frequency [Fig. 3(c)]. This oscillation bears the signatures of the $m = 1$ diocotron oscillation observed in cylindrical electron plasma experiments [19,20]. First, oscillations measured on the top and bottom probes are approximately 180° out of phase, indicating an odd poloidal mode number (e.g., $m = 1$). Second, oscillations measured with toroidally separated probes on the outboard midplane are in-phase, consistent with parallel wave number $k = 0$. Third, the frequency of the oscillations (measured in the small amplitude, growth phase) is inversely proportional to the magnetic field strength. Finally, the frequency of the oscillations decays as the trapped charge decays [Fig. 3(c)]. Data demonstrating all of the characteristics listed above can be found in the references [21]. In cylindrical electron plasmas, the $m = 1$ diocotron oscillation is a mode in which the center of charge $\mathbf{E}\times\mathbf{B}$ rotates azimuthally due to the electric field of its image charge in the grounded vacuum chamber. The frequency (at small amplitude), given by

$$f = \frac{Q}{4\pi^2 \epsilon_o L b^2 B}, \tag{1}$$

depends only on the total charge per unit length (Q/L) but not on the radial charge distribution (B is the magnetic field strength and b is the radius of the conducting wall) [22]. Using Eq. (1), the trapped charge (14 nC), the length of the plasma (225 cm), and the least squares fit of the measured frequency (at small amplitude) versus magnetic field ($f = [(378 \pm 3)/B]$ Hz T), an effective wall radius of $b \approx 22$ cm is calculated. This number is consistent with the poloidal dimensions of the vacuum chamber (44 cm by 44 cm), and further bolsters the conclusion that the observed oscillation is a toroidal version of the well-known $m = 1$ diocotron mode.

Additional confirmation of the $m = 1$ character of the observed mode is provided by the phosphor screen images of the dumped plasma. The top panel of Fig. 4 shows the signal from the bottom wall probe for times early in the trapping phase and averaged over 12 shots for which the plasma was dumped later than 0.20 ms. Fortuitous reproducibility of the phase of the oscillations relative to the initiation of trapping permits comparison of this graph with the images obtained when the plasma was dumped onto the phosphor screen at the times indicated by the dashed lines. The sequence of intensity contour plots shown in the bottom panels of Fig. 4 shows the poloidal rotation of the center of charge, completing one cycle between 0.125 and 0.170 ms.

As the amplitude of the oscillation grows the mode frequency rises slightly [Fig. 3(c)], qualitatively consistent with the nonlinear frequency shift of the large amplitude $m = 1$ diocotron mode seen in cylindrical traps [20]. The displacement of the plasma becomes comparable to or larger than the dimensions of the phosphor screen and some of the dumped plasma no longer strikes the phosphor screen. This leads to the increased scatter in the measurement of trapped charge [Fig. 3(a)] at longer trapping times. A greater or lesser fraction of the dumped plasma strikes the phosphor screen depending on the phase of the $m = 1$ oscillation at the time of the dump. The observation that the charge begins to fall earlier than the mode frequency [compare Figs. 3(a) and 3(c)] is also due to this same effect. The confinement time is therefore better estimated by the fall-off in the diocotron mode frequency (≈ 2.0 ms) rather than the measured charge decay time (≈ 1.4 ms).

In cylindrical traps, the $m = 1$ mode is stable but can be made unstable using a resistive wall [19]. Wall resistivity, toroidal effects [6], or the ion resonance instability [23–25] may account for the unstable nature of the mode in the torus, and this is a subject of ongoing investigation. However, the mode is amenable to feedback stabilization given its low frequency and long wavelength structure as has been demonstrated in cylindrical traps [26]. When the signal from one of the wall probes is phase shifted, amplified, and applied to the inner middle horizontal field electrode (Fig. 2), the mode is successfully suppressed. The resulting confinement is enhanced by an order of magnitude to 18 ms. Figure 5 shows the dumped charge versus trapping time both with feedback applied (triangles) and without feedback applied (crosses). The latter data points are identical to those shown in Fig. 3(a). When feedback is applied, the trapped charge increases during the first 4 ms (Fig. 5). This observation is consistent with fueling of the electron population by ionization of the residual gas and with the speculation that the ion resonance instability may be responsible for mode growth(without feedback). The order of magnitude improvement resulting from the application of feedback confirms that, without feedback, particle losses result from the growth of the diocotron mode to large amplitude, causing electrons to scrape-off on material surfaces.

We compare our results to the empirical confinement scaling results of Driscoll and Malmberg, $\tau = 1.6 \times 10^{-2}[L(\mathrm{cm})/B(G)]^2$, obtained in their early cylindrical trap [27]. For an experiment 225 cm long with a 196 G magnetic field, the Driscoll-Malmberg scaling relation yields a 12 ms confinement time. Since we obtain confinement times slightly longer than 12 ms, we conclude that no unexpected toroidal effects are present on the millisecond time scale. We make no claim that confinement in our experiment is limited by the same mechanism that limited confinement in the cylindrical experiments. We use the comparison to benchmark progress in the effort to confine toroidal electron plasmas. In fact, initial calculations indicate that, whereas transport in the experiments of Driscoll and Malmberg was due to field asymmetries, transport due to electron-neutral collisions should be significant in the present experiment on the time scale of tens of milliseconds because of the relatively high neutral pressure ($\approx 5 \times 10^{-7}$ Torr). Future measurements of confinement scaling with magnetic field and neutral pressure will determine whether trap

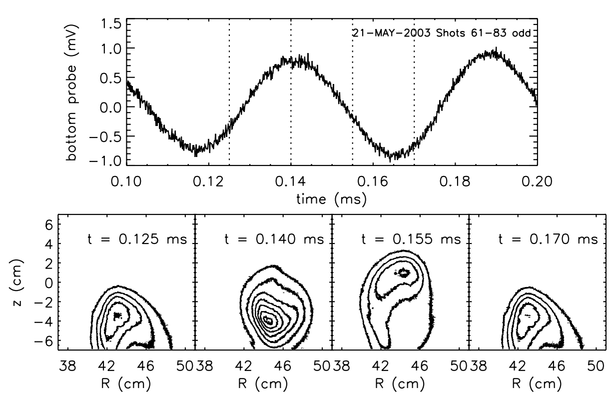

FIG. 4. A 12-shot average of the bottom wall probe signal (top panel) showing the 4 times (vertical dashed lines) at which the plasma was dumped to generate the phosphor intensity contour plots (bottom panels).

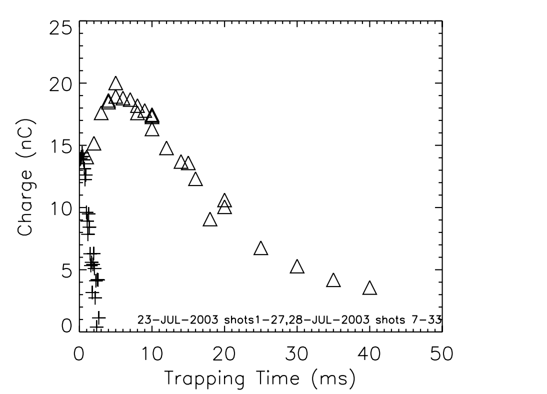

FIG. 5. A comparison of the trapped charge versus trapping time with feedback on the $m = 1$ diocotron signal (triangles) and without feedback (crosses).

asymmetries, electron-neutral collisions, or some other effect limits confinement to 18 ms in the present device.

To assess whether equilibrium has been established, the confinement time is compared to the longest characteristic time scale for single-particle motion. The characteristic time scales for single-particle motion, ordered from shortest to longest, are the cyclotron period (1.8 ns), the $\mathbf{E}\times\mathbf{B}$ rotation period ($\approx 2.7\ \mu$s), the toroidal bounce time (0.8–7.6 μs), and the cross-field drift transit time due to curvature and ∇B drifts (20–200 μs). The latter two time scales depend on the energy spread or effective temperature of the plasma. Temperature is not measured in the present experiment, but realistic considerations place it within the bounds from 1 to 100 eV. On the lower end, the turn-to-turn potential difference on the imperfectly wound spiral tungsten filament is about 10 V, leading us to expect that the energy spread is likely to be of this order of magnitude. On the upper end, there are theoretical reasons for expecting rapid particle loss if the typical single-particle kinetic energy is greater than the space-charge potential [14]. Using the very conservative range of possible values for the effective temperature, the longest characteristic single-particle time scale (200 μs) is almost 2 orders of magnitude shorter than the observed confinement time (18 ms). The results presented here, therefore strongly support the existence of an equilibrium in which the poloidal $\mathbf{E}\times\mathbf{B}$ drift acts as an effective rotational transform for the toroidal electron plasma. The same range of possible temperature values also yields a range of Debye lengths from 0.3 cm ($T = 1$ eV) to 3.0 cm ($T = 100$ eV). The minor radius of the plasma (5 cm) is therefore larger than the Debye length.

In summary, a partially toroidal trapping scheme has been employed to permit rapid charge injection along field lines tied to the trapping region, generating the poloidal $\mathbf{E}\times\mathbf{B}$ rotation necessary to provide an equilibrium state. Confinement times as long as 18 ms are achieved; they are almost 2 orders of magnitude longer than previous electron plasma experiments with a purely toroidal field. The longest confinement times are achieved through the application of feedback to suppress the growth of the $m = 1$ diocotron mode. In the absence of feedback, confinement is limited (to 2 ms) by the growth of the oscillation to large amplitudes whereupon electrons are lost to material surfaces.

We acknowledge the assistance of F. Anderegg in the design of the feedback experiment. The project is funded by Lawrence University and by grants from Research Corporation (No. CC4593) and the U.S. Department of Energy (No. DE-FG02-98ER54503).

[1] Thomas M. O'Neil, Phys. Today **52**, No. 2, 24 (1999).
[2] J. D. Daugherty and R. H. Levy, Phys. Fluids **10**, 155 (1967).
[3] K. Elsässer, M. Y. Yu, and P. K. Shukla, Phys. Lett. A **152**, 59 (1991).
[4] K. Avinash, Phys. Fluids B **3**, 3226 (1991).
[5] O. A. Hurricane, Phys. Plasmas **5**, 2197 (1998).
[6] S. N. Bhattacharyya and K. Avinash, Phys. Fluids B **4**, 1702 (1992).
[7] T. M. O'Neil and R. A. Smith, Phys. Plasmas **1**, 2430 (1994).
[8] J. D. Daugherty, J. E. Eninger, and G. S. Janes, Phys. Fluids **12**, 2677 (1969).
[9] M. Mohri, M. Masuzaki, T. Tsuzuki, and K. Ikuta, Phys. Rev. Lett. **34**, 574 (1975).
[10] W. Clark, P. Korn, A. Mondelli, and N. Rostoker, Phys. Rev. Lett. **37**, 592 (1976).
[11] A. Fisher, P. Gilad, F. Goldin, and N. Rostoker, Appl. Phys. Lett. **37**, 531 (1980).
[12] Puravi Zaveri, P. I. John, K. Avinash, and P. K. Kaw, Phys. Rev. Lett. **68**, 3295 (1992).
[13] S. S. Khirwadkar, *et al.*, Phys. Rev. Lett. **71**, 4334 (1993).
[14] M. R. Stoneking, P. W. Fontana, R. L. Sampson, and D. J. Thuecks, Phys. Plasmas **9**, 766 (2002).
[15] H. Himura, C. Nakashima, H. Saito, and Z. Yoshida, Phys. Plasmas **8**, 4651 (2001).
[16] C. Nakashima *et al.*, Phys. Rev. E **65**, 036409 (2002).
[17] Thomas Sunn Pedersen and Allen H. Boozer, Phys. Rev. Lett. **88**, 205002 (2002).
[18] J. H. Malmberg and C. F. Driscoll, Phys. Rev. Lett. **44**, 654 (1980).
[19] W. D. White, J. H. Malmberg, and C. F. Driscoll, Phys. Rev. Lett. **49**, 1822 (1982).
[20] K. S. Fine, C. F. Driscoll, and J. H. Malmberg, Phys. Rev. Lett. **63**, 2232 (1989).
[21] M. R. Stoneking, M. A. Growdon, M. L. Milne, and R. T. Peterson, in *Non-Neutral Plasmas V*, edited by M. Schauer, T. Mitchell, and R. Nebel (American Institue of Physics, New York, 2003), p. 310.
[22] Ronald C. Davidson, *Physics of Nonneutral Plasmas* (Addison-Wesley, Redwood City, CA, 1990), p. 306.
[23] R. H. Levy, J. D. Daugherty, and O. Buneman, Phys. Fluids **12**, 2616 (1969).
[24] J. Fajans, Phys. Fluids B **5**, 3127 (1993).
[25] A. J. Peurrung, J. Notte, and J. Fajans, Phys. Rev. Lett. **70**, 295 (1993).
[26] J. H. Malmberg *et al.*, in *Non-Neutral Plasma Physics*, edited by C. W. Roberson and C. F. Driscoll (American Institute of Physics, New York, 1988), p. 28.
[27] C. F. Driscoll and J. H. Malmberg, Phys. Rev. Lett. **50**, 167 (1983).